

A Multi-Stage Fuzzy Logic Controller for Hybrid-AC Grid-Battery Charging Drive System

Abdel-Fattah Attia^{1,3}, Adel Mahmoud Sharaf^{2,3,*}, Fathalla Selim¹

¹ Faculty of Engineering, Kafrelsheikh University, Kafrelsheikh, Egypt

² Sharaf Energy Systems, Inc. Fredericton, NB, Canada

³ Intelligent System Research Group (ISRG), Kafrelsheikh University, Kafrelsheikh, Egypt

Received: 14 November 2019; Revised: 01 December 2019; Accepted: 12 December 2019; Published: 31 December 2019

Turk J Electrom Energ Vol.: 4 No: 2 Page: 1-12 (2019)

SLOI : <http://www.sloi.org/>

*Correspondence E-mail : profdrasharaf@yahoo.ca; aheliel@eng.kfs.edu.eg

ABSTRACT The paper presents a fuzzy logic modified multi-stage hierarchical Fuzzy Logic PID Control Scheme for hybrid AC Grid-Drive-Battery Charging System. The multistage control scheme includes two fuzzy control stages for the separate PD and PID parts to ensure fast dynamical response, robust and effective speed control and efficient energy utilization with minimal ripple currents and transient over voltages during battery charging. The scheme ensures effective robust reference speed tracking of the dc PMDC motor drive with minimal transient currents and excursion voltage conditions. The use of dc side green plug and switched capacitor filters ensures effective stabilized damping and optimized performance on both dc and ac sides of the utilization hybrid AC-DC scheme. Dynamic speed regulation is enhanced by the introduced DC and AC filters regulated by multistage fuzzy logic multi loop controllers. AC side Switched Filter-Voltage stabilization is fully effective to ensure decoupled AC-DC operation and improved energy utilization and power factor enhancement.

Keywords: Hybrid AC-DC Drive-Battery Charging Scheme, Switched Filter-Compensation using-level Fuzzy Logic Controller

Cite this article as: A-F. Attia, A. M. Sharaf, F. Selim, A Multi-Stage Fuzzy Logic Controller for Hybrid-AC Grid-Battery Charging Drive System, Turkish Journal of Electromechanics & Energy, 4(2), 1-12, (2019).

1. INTRODUCTION

Different techniques and methods are utilized in DC motor drives with added battery charging schemes. The following section discusses the key control structures:

List of symbols

Symbol	Definition
PID	Proportional-Integral-Derivative
PV	Photovoltaic
PMDC	Permanent Magnet Dc motors
LQR	Linear Quadratic Regulator
PSO	Particle Swarm Optimization
SA	Simulating Annealing
FLC	Fuzzy Logic Controller
HFLC	Hierarchical Fuzzy Logic Control
GPFC	Capacitor-Green Power Filter Compensator
PMSM	Permanent Magnet Synchronous Motor
PMDC	Permanent Magnet DC Motor

1.1. PID controller tuning

There are many types of drive system controllers, such as the linear quadratic regulator (LQR) associated with the clipped optimal algorithm, a dynamic inverse model using nonlinear autoregressive exogenous (NARX)-type artificial neural networks, and algorithms based on fuzzy logic [1]. Nevertheless, the conventional proportional-integral-derivative (PID) type controller is the most common form of feedback and the best controller used in practice [2,3]. The gain parameters can be tuned using any of heuristic methods such as genetic algorithms (GA) [4], particle swarm optimization (PSO) [5, 6], Tabu search (TS) [7], simulating annealing (SA) [8] and Ant colony optimization algorithms [9]. However, the conventional PID controllers generally do not work well for nonlinear systems [10]. Fuzzy Logic Controller (FLC) is another alternative that can be used to handle these problems. In literature, several studies adopted FLC and PID while some used FLC for adaptation of a conventional PID controller [11] where a FLC uses error signal and dynamic derivative change of error to optimize the controller gains. Another study concerned

with the relation of input/output of PID based on FLC structure [12]. The suggested article uses a multistage FLC controller (HFLC) to control PID comments to focus on relative feedback derived separately from integrated feedback. The controller HFLC contains parallel and series stages of the output and inputs [11].

1.2. Driving systems

Electric Vehicles (EV) are propelled by different types of DC and AC motor drives and are powered by rechargeable battery systems. It used Photovoltaic (PV) for charging AC and DC Motor Drives which have numerous advantages of efficient, high torque/high speed controllable mode with fast acceleration with no pollution or adverse environmental effects in comparison to petrol/diesel/NG powered electric vehicles [13]. The electric converter interface power electronics and switching strategies with flexible/adaptive/dynamically controlled gains can ensure that efficiency, reliability, robust speed/torque control and fast acceleration but all are hampered by the current battery technology and charge limitations. Battery charging requirements and impact on the host electric grid still pose a limiting factor in case of massive electric vehicle penetration levels [14]. Some studies aimed to improve the battery charging efficiency by many types of controlling using MATLAB/Simulink various models [15]. There are many researches deal with EV with many types of controller such as, a four-wheel EV where the source of power is acquired from battery and also from solar energy was controlled by PIC Micro-controller [16]. In another study, researchers have demonstrated the possibility of an improved four wheels' vehicle stability which utilizes four independent driving wheels for motion by using the adaptive fuzzy logic controller rather than classical PI controller [17].

PID tri-loop controller used for a hybrid PVFC diesel-battery powered all-wheel drive electric vehicle using four (PMDC) motors is introduced in [18, 19, 28]. In paper [20], Authors introduced similar basic theories as in [18, 19] on four-wheel electric vehicle but based on a permanent magnet synchronous motor (PMSM). The main contributions of the article can be highlighted as follows:

- The paper presents a fuzzy logic modified multi-stage hierarchical fuzzy logic PID control scheme for hybrid AC grid-drive-battery charging system.
- The multistage control scheme includes two Fuzzy control stages for the separate PD and PID parts to ensure a fast-dynamical response.
- This novel approach reduces the fuzzy rule numbers but still maintains the linguistic meaning of fuzzy variables.
- The scheme ensures effective robust reference speed tracking of the DC PMDC motor drive with minimal transient currents and excursion voltage conditions.
- It presents a dynamic and efficient decoupled AC-DC hybrid smart-grid-drive-battery charging scheme using type D-four-quadrant DC chopper control.
- The flexible multi charging strategy used a multi loop dynamic controller to adjust the (V-I-P) Charging selected weighted modes in to ensure fast charging with minimal transient voltages and inrush current

conditions and for PMDC motor speed control related to other studies.

The rest of the paper introduces the, all-wheel drive system description. Then, the proposed Hierarchical Fuzzy Logic Controller (HFLC) is explained. The system simulation of the proposed control technology under different operating conditions precedes the discussion of findings and conclusions.

2. PMDC-DRIVE SYSTEM DESCRIPTION

The study comprises a hybrid AC-DC scheme for battery charging and PMDC motor drive system using a four Quadrant DC-DC Converter Stage (Type-D Chopper). The use of the three phase SFC on AC side as a hybrid tuned arm filter and reactive compensator is facilitated by complementary PWM switching of the solid-state switches. The GPFC, green plug located in the DC side is a switched energy storage and dynamic filtering stage to reduce transients and inrush conditions on the DC side. The DC boost chopper switched at higher frequency endure fast battery charging with minimized inrush conditions that creates low energy utilization and power factor reduction at the AC interface. The common DC bus scheme is stabilized using a novel low-cost switched capacitor-green power filter compensator (GPFC) [19, 26] and [29]. The sinusoidal pulse modulation technique is utilized for duty cycle ratio modulation of the two basic multi-loop error driven regulation schemes, namely:

- Speed reference tracking controller
- Switched filter-GPFC DC bus voltage stabilization and inrush current damping controller.
- Both AC-DC side regulators utilizes the multi-tier hierarchical fuzzy logic control scheme to ensure optimal on-off switching of pulse width modulation stages to ensure effective speed reference tracking with minimal overshoot/undershoot and transient inrush currents under PV-DC source excursions and insolation level/temperature variations.

Figure 1 depicts the Hybrid AC-DC Scheme smart grid interface. It comprises the AC grid interface to DC side using a diode rectifier bridge stabilized by a switched filter - capacitor compensators:

The AC side power factor and power quality is enhanced using SPWM-complementary switching of a tuned arm LC-filter and capacitive compensator.

The DC green plug filter is used to reduce current ripples in rush current conditions created by fast inrush motor operation and battery charging. A boost- type DC- DC converter (chopper) is controlled to ensure fast efficient energy utilization with reduced current/voltage transient excursions during motor start/stop and battery charging/discharging modes.

The multi-loop error driven time descaled controllers are self-adjusted by selection of loop weightings and loop descaled time for decoupled regulator operation to ensure time descaling and effective weighting for fast dynamic control. The use of GPFC in DC common bus as a pre-stage to boost chopper endures combined fast switching with reduced inrush currents and stabilized DC common bus. The Figure 1 also shows the micro grid supply with the hybrid PV and AC source with the backup battery. The following list are definitions,

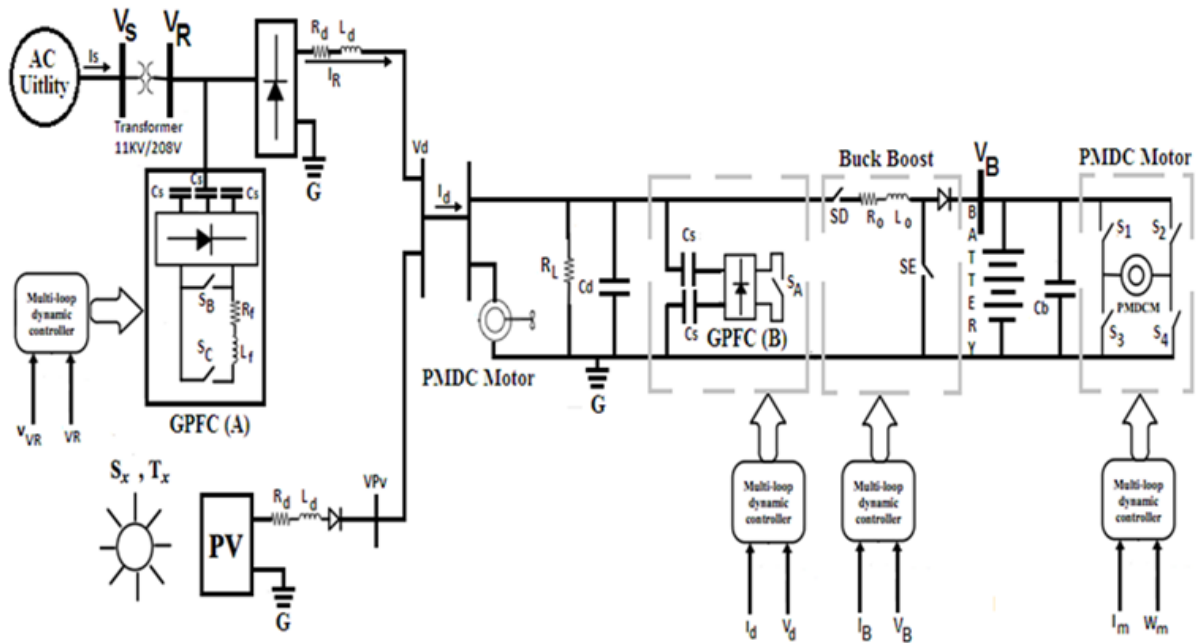


Fig. 1. Hybrid AC-DC Grid PV PMDC Drive Battery Charging Scheme.

- AC source control regulator uses six Pulse controlled diode rectifiers.
- AC/DC converter is utilized to regulate the voltage at AC bus and limit inrush current conditions.
- The green plug filter compensator has a PWM switching that ensures power quality, efficient operation and ripple free switching transients and inrush current conditions. The dual action Buck-Boost converter controller regulates the PWM switching to ensure voltage regulation.
- The PMDC motor drive system is controlled to ensure dynamic fast tracking of reference speed as well as reduced ripple content with efficient energy utilization of the PV array Lithium- ion battery (Li-ion) battery hybrid source.

3. THE HIERARCHICAL FUZZY LOGIC CONTROL (HFLC) STRUCTURE

The structure of the two cascaded-stage PID controller is similar as the PID controller as illustrated in Figure 2. The design of the multi- stage fuzzy PID controller begins with the design of PDFLC. Integrated feedback is integrated with the fuzzy switch to form PIDFLC, after improving the PDFLC. The designing of the fuzzy controller is started by selecting input and output variables to represent (PDFLC). The next step is to use PIDFLC to output the PDFLC stage and integrate the error ($\int e$) as input-variables.

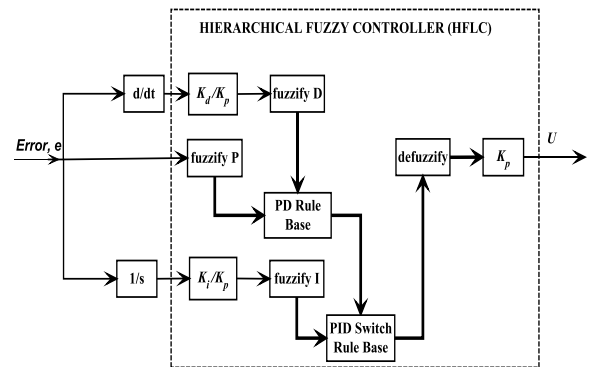


Fig.2. Multi-stage fuzzy PID controller

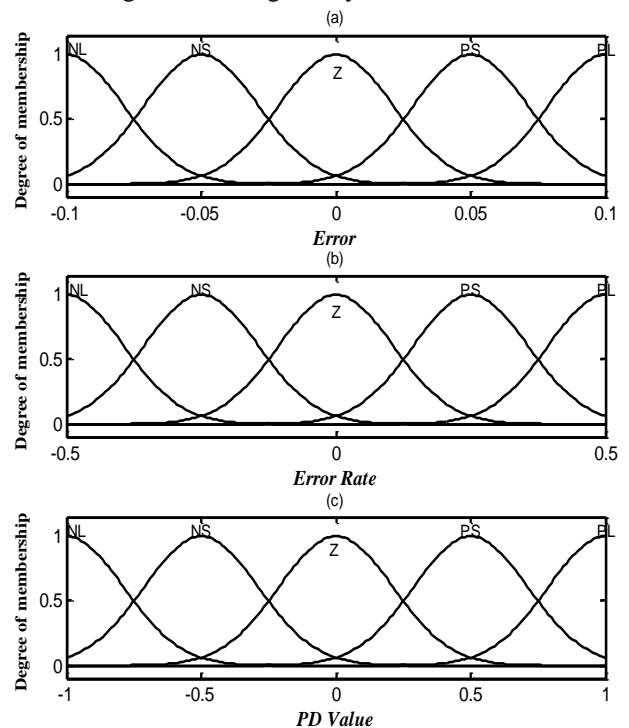


Fig.3. Normalized membership functions for I/O variables of PDFLC.

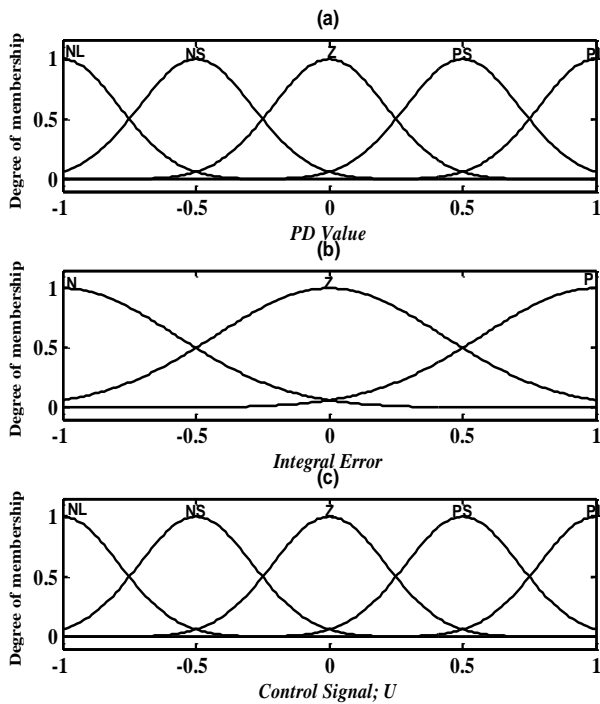


Fig.4. Normalized membership functions for I/O variables of PIDFLC.

Each variable is accompanied by key inputs, and for PDFLC using Five-Gaussian membership functions as shown in Figure 3. The PD value represents PDFLC output by five membership functions as described in Figure 3 and 4. The base rule are 25 rules are listed in Table 1, are also defined for PDFLC. Decision-rules have a general shape: If e is NS and \dot{e} is Z then PD value is NS. Where the membership functions (mf) is defined as follows: $mf_j \in \{NL, NS, Z, PS \text{ and } PL\}$.

Table 1. PDFLC rule base

The global error; e

		NL	NS	Z	PS	PL
Error rate; \dot{e}	NL	NL	NL	NL	NS	Z
	NS	NL	NL	NS	Z	PS
	Z	NL	NS	Z	PS	PL
	PS	NS	Z	PS	PL	PL
	PL	Z	PS	PL	PL	PL

Table 2. PIDFLC rule base.

Integral Error; $\int e$

		N	Z	P
PD Value	NL	NL	NL	NS
	NS	NS	NS	Z
	Z	Z	Z	Z
	PS	Z	PS	PS
	PL	PS	PL	PL

The PID-FLC regulation scheme using a decision-table based on two input variables PD value which is the cascaded output of PDFLC plus the error integrator $\int e$. The PD input variable uses five fuzzy sets. The second input is also evaluated through three fuzzy sets. The PID-FLC can be illustrated as given in Table 2. Figure 5

and 6 depict the surface rule viewers for the two stage-controllers; PDFLC and PIDFLC respectively. The full decision rules are reduced to 40 instead of 125 for the classical FLC method used for three input variables.

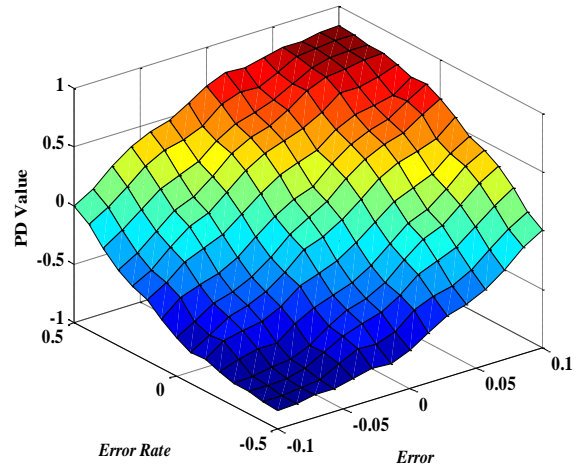


Fig.5. Surface view of rules for the PDFLC controller.

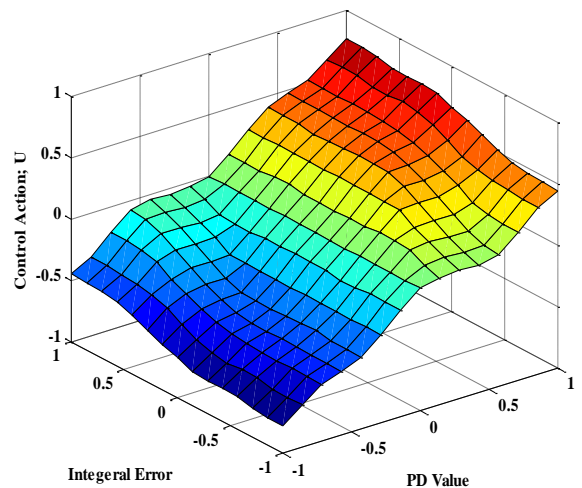


Fig.6. Surface view of rules for the PIDFLC.

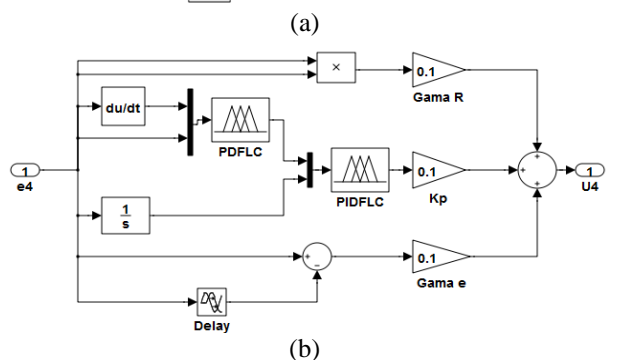
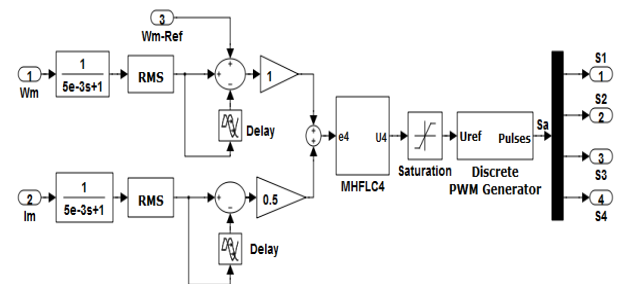


Fig.7(a) Dual-loop error driven error scaled -weighted-modified HFLC controller for PMDC motor drive, (b) Novel weighted-modified HFLC dynamic controller with error squared and rate compensation loops.

3.1. Dynamic Error Driven Control

The dynamic error driven controller is developed and used in [22], [23] and [24]. The novel dynamic error HFLC is implanted for speed control of PMDC motors that comprises two basic loops as shown in Figure 7. Figure 8 shows the error and change of error curves as input variables whereas PD value represents output for PDFLC4 controller; respectively. The PD value speed error (e_4), integral speed error represents the variable inputs for 2nd stage controller; PIDFLC4 as shown in Figure 9. Figure 10 depicts a modified two stage dual-loop error driven HFLC controller using a switched filter compensation green plug scheme GPFC for ripple reduction, inrush current minimization, AC side power quality and decoupled AC-DC operation as well as efficient utilization of energy supplied by PV array with Lithium- ion battery (Li-ion) battery back-up source.

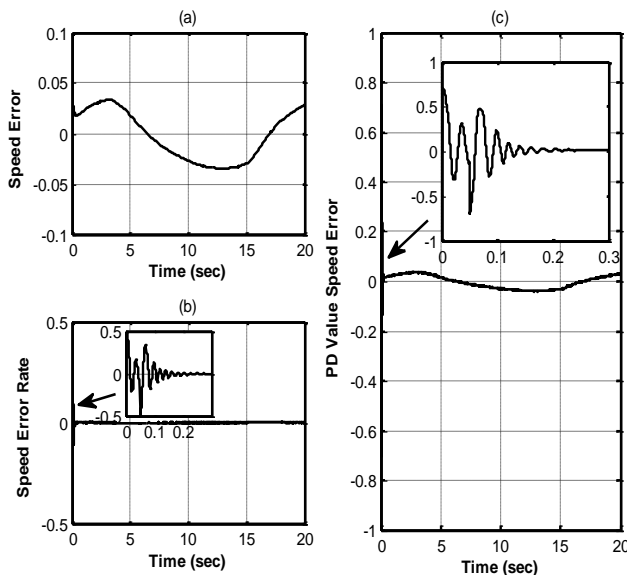


Fig.8. (a) and (b) represent input variables whereas (c) represents output for PDFLC4 controller; respectively.

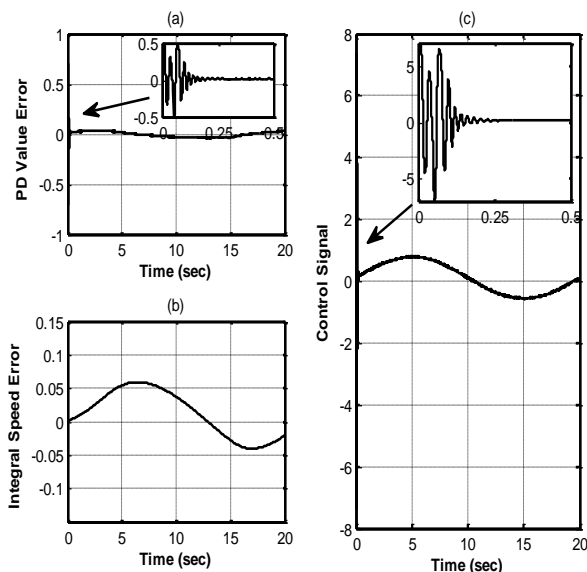


Fig.9. (a) and (b) represent input variables whereas (c) represents output for PIDFLC4 controller; respectively.

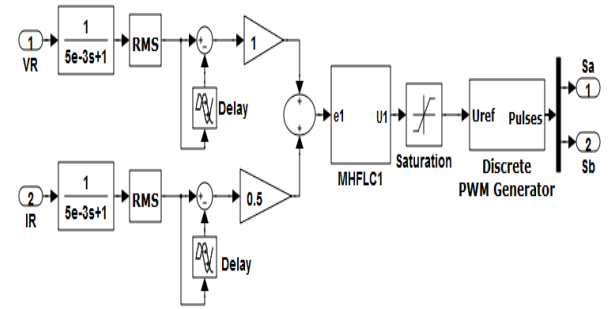


Fig.10. Dual-loop error driven weighted-modified dual-loop error driven HFLC1 controller for the AC side SFC Filter-Compensator (A).

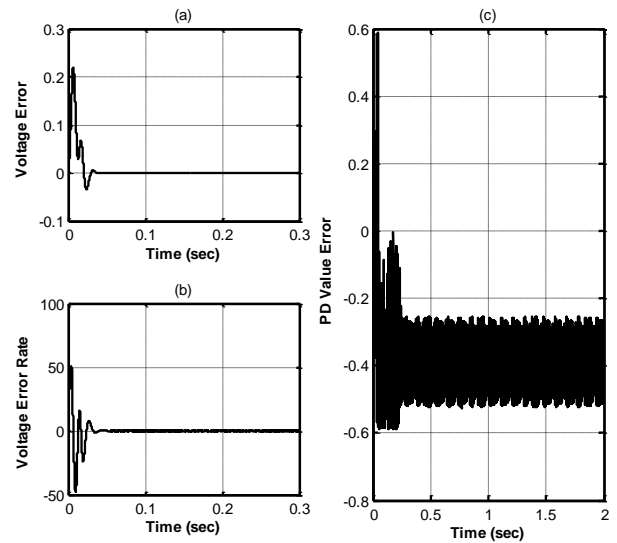


Fig.11. (a) and (b) represent input variables whereas (c) represents output for PDFLC1 controller; respectively.

Figure 11 shows the error and change of error curves as input variables whereas PD value of voltage error represents output for PDFLC1 controller, respectively. The PD value of voltage error (e_1), integral voltage error represents the variable inputs for 2nd stage controller; PIDFLC1 as shown in Fig. 12.

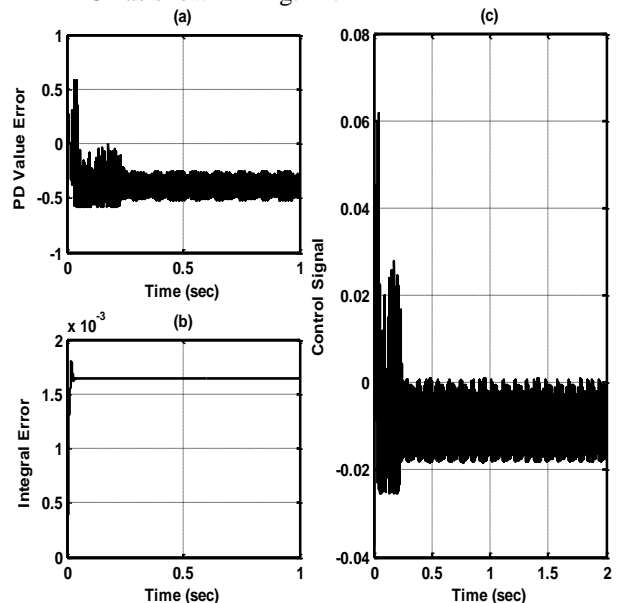


Fig.12. (a) and (b) represent input variables whereas (c) represents output for PIDFLC1 controller; respectively.

The PIDFLC1 controller is shown in Figure 12. The Filter-Green Plug GPFC controller used a decoupled weighted time de-scaled loop. The new GPFC design is connected across the DC bus terminal to stabilize the common DC bus voltage in order to allow efficient ripple free operation using two decoupled control loops as shown Figure 13.

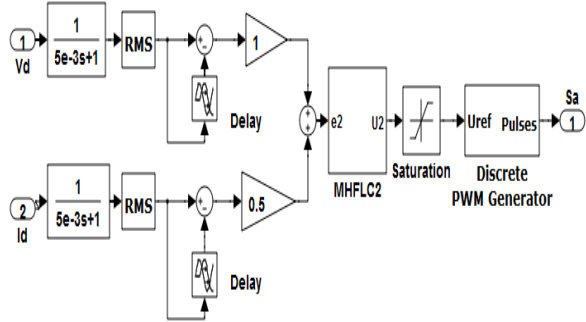


Fig.13. Dual-loop error driven weighted-modified dual-loop error driven HFLC2 controller for common DC Bus GPFC (B).

The Bus voltage is used as input to loop 1 (as an error difference from reference value), the error (e_2) is used for voltage stabilization. The input to loop 2 is the bus current [25, 27]. Figure 14 shows the error and change of error curves as input variables whereas PD value of voltage error represents output for PDFLC2 controller; respectively. The PD value of voltage error (e_2), integral voltage error represents the variable inputs for 2nd stage controller; PIDFLC2 as shown in Figure 15.

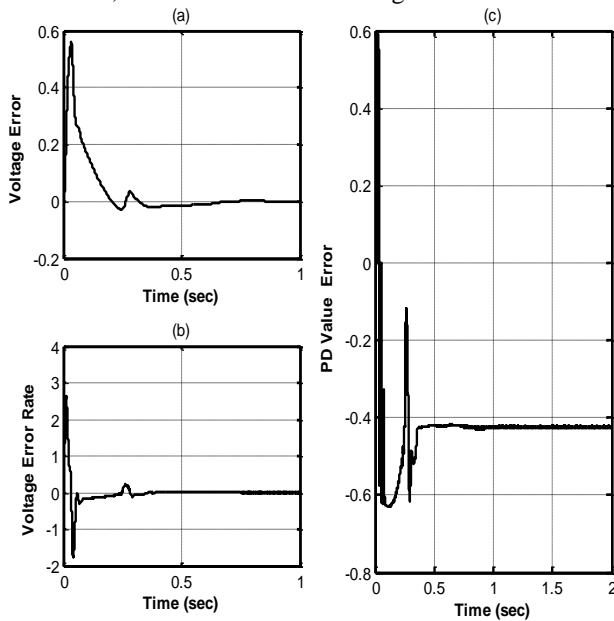


Fig.14. (a) and (b) represent input variables whereas (c) represents output for PDFLC2 controller; respectively.

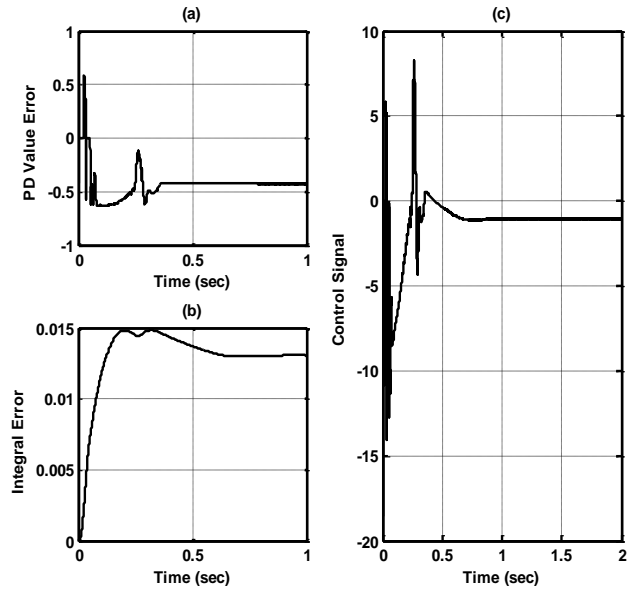


Fig.15. (a) and (b) represent input variables (c) represents output for PIDFLC2 controller; respectively.

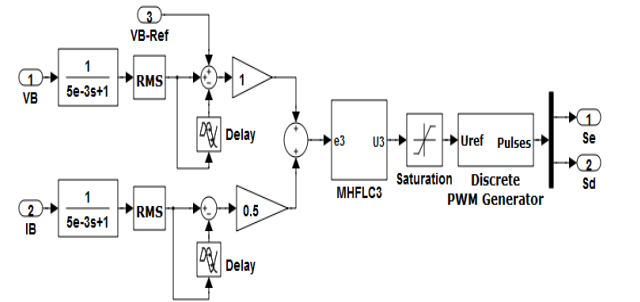


Fig.16. Dual-loop error driven weighted-modified dual-loop error driven HFLC3 controller for DC Buck-Boost type DC-DC Converter.

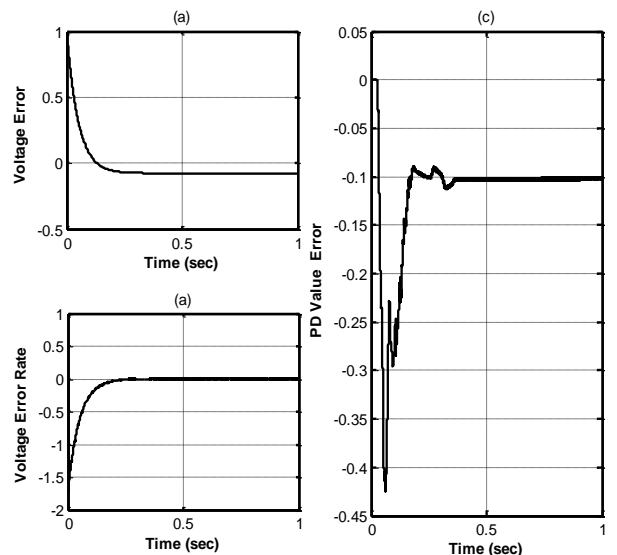


Fig.17. (a) and (b) represent input variables whereas (c) represents output for PDFLC3 controller; respectively.

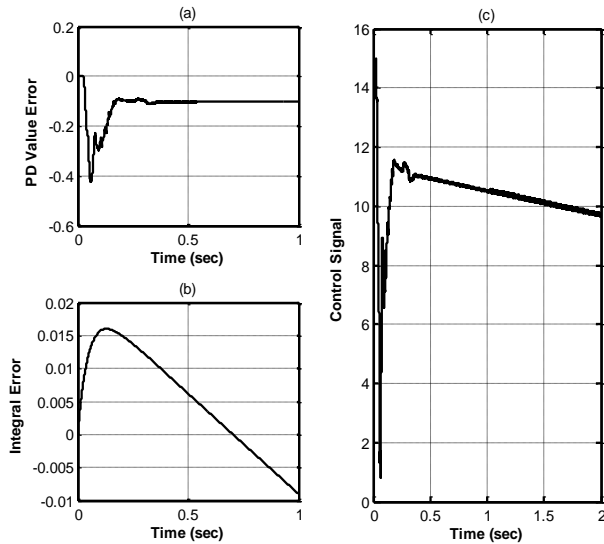


Fig.18. (a) and (b) represent input variables whereas (c) represents output for PIDFLC3 controller; respectively

Figure 16 shows the novel modified HFLC controller is implemented to control buck-boost converter. Figure 17 shows the error and change of error curves as input variables whereas PD value of voltage error represents output for PDFLC3 controller; respectively. The PD value of voltage error (e_3), integral voltage error represents the variable inputs for 2nd stage controller; PIDFLC3 as shown in Figure 18.

4. DIGITAL SIMULATION RESULTS AND DISCUSSION

The novel dual-loop dynamic weighted modified HFLC dynamic controllers are validated for voltage stabilization and dynamic reactive compensation using MATLAB/Simulink/Simpower toolbox software environment. The effectiveness of the HFLC controllers were validated for different speed trajectories (step references, ramp and sinusoidal references) with dissimilar loading conditions and parameters.

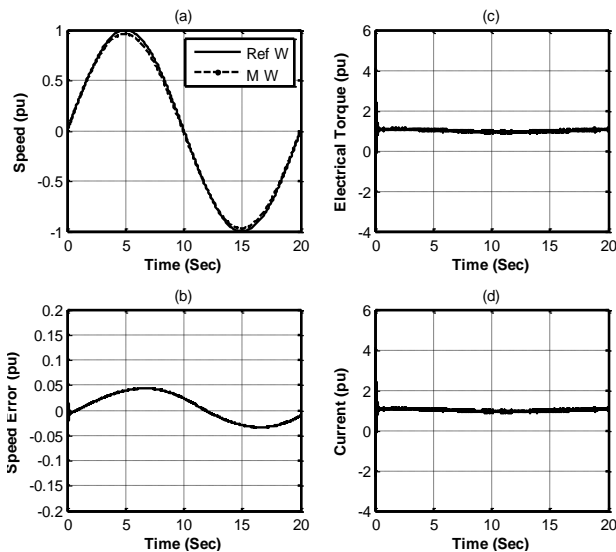


Fig.19. (a) Dynamic speed reference response of PMDC motor, (b) speed error vs. time, (c) Electrical torque vs time, (d) Motor current vs. time.

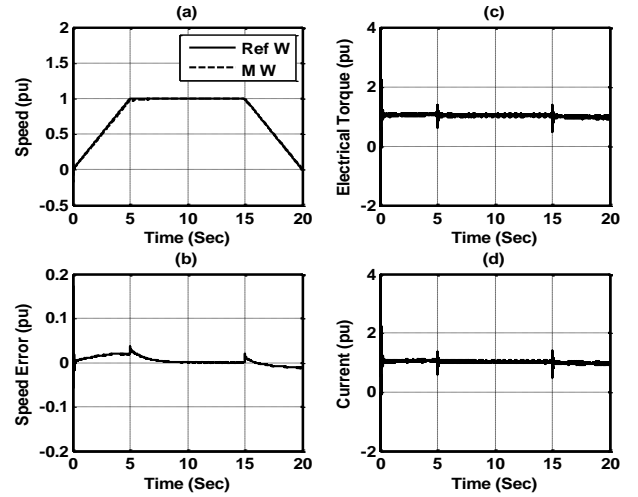


Fig.20. (a) Dynamic speed reference response of PMDC motor, (b) Speed error vs time. (c) Electrical torque vs time. (d) Motor current vs time.

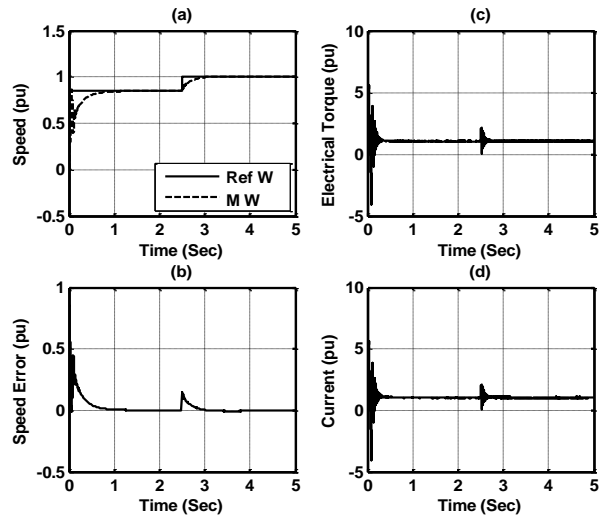


Fig. 21. (a) Dynamic speed reference response of the PMDC motor. (b) Speed error vs. time. (c) Electrical torque vs. time. (d) Motor current vs. time.

The hybrid smart grid photovoltaic V2G scheme is validated for load changes, photovoltaic Insolation and temperature changes. Figures 19(a), 20(a) and 21(a) show the system dynamic response for different reference speed trajectories. In the same time, Figures 19(b), 20(b) and 21(b) show the error for different reference speed trajectories. In addition, the Figures 22, and 23 show the system dynamic response for the AC source. Figs. 19(c), 20(c), and 21(c) show the electrical torque for the PMDC motor. Figs. 19(d), 20(d) and 21(d) show the PMDC motor current I_m .

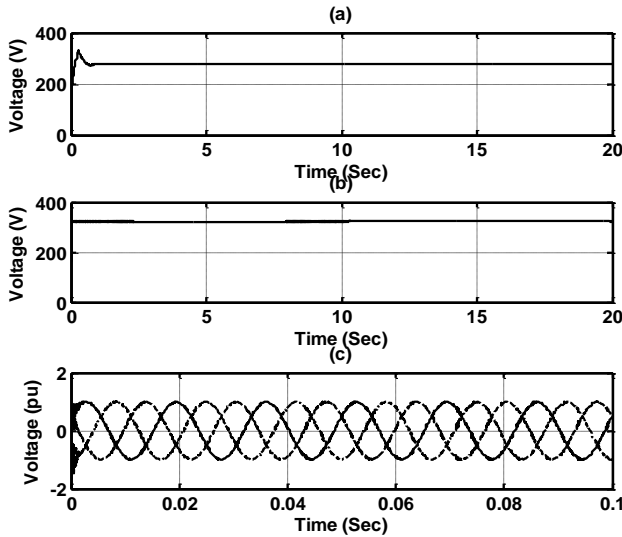


Fig. 22. (a) DC side Voltage VD at VD Bus. (b) The Voltage VB at VB Bus. (c) The Voltage at the AC Source VS Bus.

The hybrid smart grid photovoltaic V2G scheme is validated for load changes ($\pm 50\%$ step changes). Figures 24 shows speed, electrical torque and current of the PMDC motor under changing of T_m . The dynamic filter green plug filter compensator with tuned controller and weighting parameters did highly improve the AC and DC bus dynamic power quality.

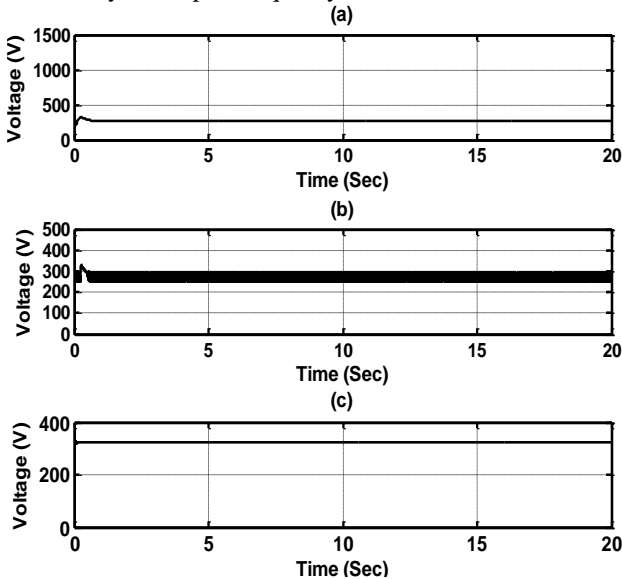


Fig.23. (a) The voltage VPV at VPV bus. (b) The voltage VR at VR bus. (c) The voltage VB at VB bus.

The unified AC-DC micro-grid V2G-DC motor drive system is controlled using the novel decoupled de-scaled error driven regulators for GPFC. Dynamic simulation results validated the modified design of the HFCLC controller to be more effective compared to modified PID controller in damping voltage transients and reduce current inrush conditions. The controller effectiveness in tracking different speed reference trajectories were tested for step reference changes and different, and other trajectory (step references, ramp and sinusoidal references) as shown in Figures. 19(a), 20(a), and 21(a).

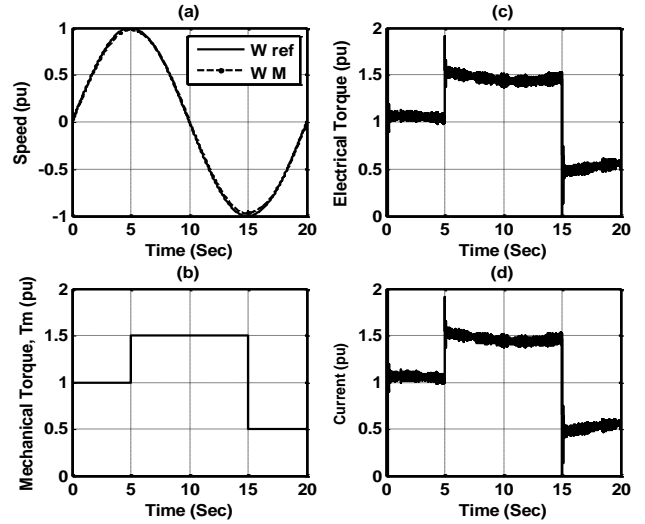


Fig.24. PMDC under load changes; $\pm 50\%$ Step changes: (a) Speed responses vs Time. (b) Mechanical Torque vs Time. (c) Electrical Torque vs Time. (d) Motor Current vs Time.

$|Re|$ is the magnitude of the hyper-plane error excursion vector for MHFLC1, MHFLC2, MHFLC3 and MHFLC4 are described by the following equations:

$$Re_1 = \sqrt{e_1^2 + \left(\frac{de_1}{dt}\right)^2}, \quad (1)$$

$$Re_2 = \sqrt{e_2^2 + \left(\frac{de_2}{dt}\right)^2}, \quad (2)$$

$$Re_3 = \sqrt{e_3^2 + \left(\frac{de_3}{dt}\right)^2}, \quad (3)$$

$$Re_4 = \sqrt{e_4^2 + \left(\frac{de_4}{dt}\right)^2}, \quad (4)$$

Figures 25 and 26 illustrate responses of HFCLCs error, controller error rate and magnitude of the hyper-plane error excursion vector for MHFLC1 and MHFLC2, MHFLC3 and MHFLC4 respectively. Figure 27 illustrates the Phase portrait for responses of error and error rate for MHFLC1, MHFLC2, MHFLC3 and MHFLC4 controllers.

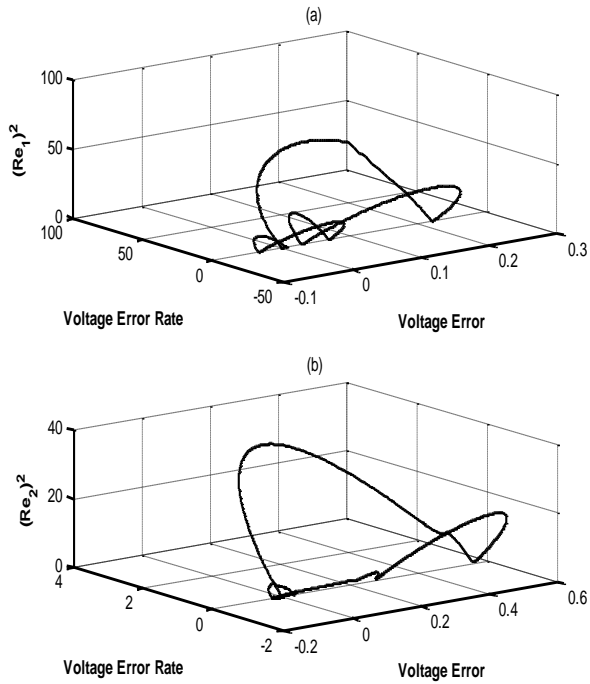


Fig. 25. 3D responses for voltage error and error rate vector for MHFLC1 and MHFLC2, respectively.

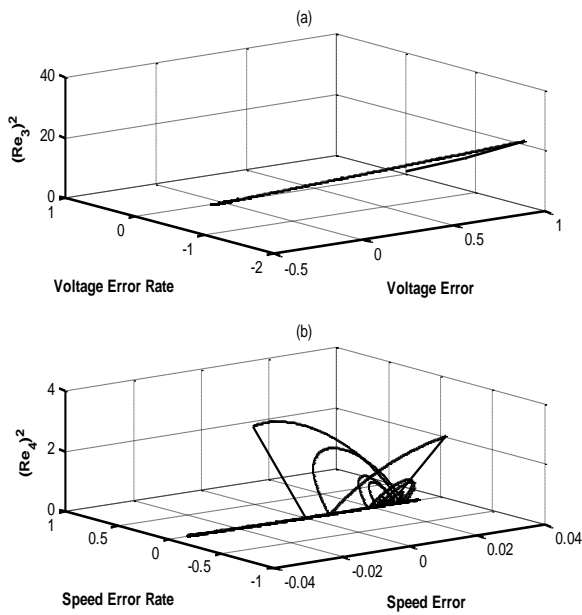


Fig.26. 3D responses for voltage error and error rate vector for a) MHFLC3; b) for MHFLC4

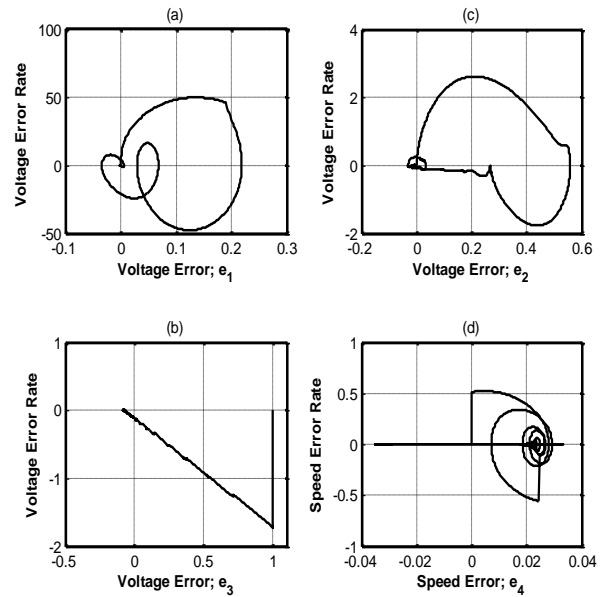


Fig.27. Phase portrait for Responses of error and error rate a) for MHFLC1, b) for MHFLC2, c) for MHFLC3, d) for MHFLC4 controllers.

In addition, the Figure 28 and Figure 29 show short circuit and open circuit at the input to the AC side. AC open circuit fault for 20 ms and the short circuit fault for 120 ms for both VR and IR as illustrated in Figure 28 and Figure 29.

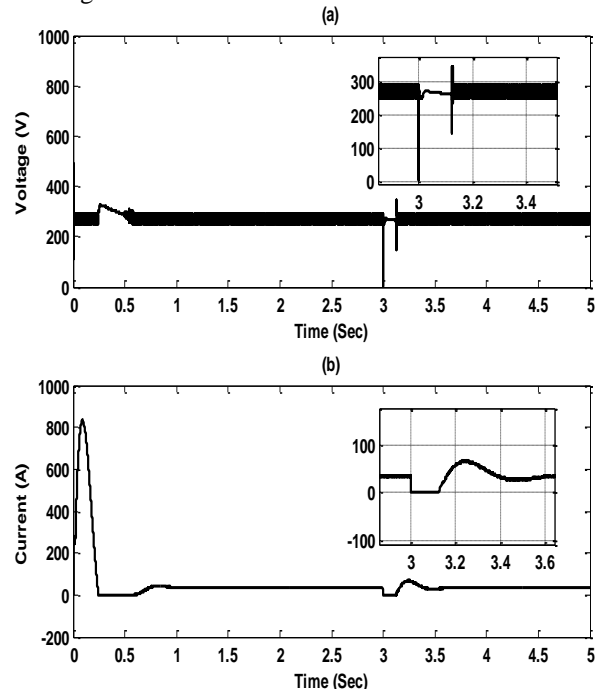


Fig.28. (a) The voltage VR at AC bus under the short circuit fault. (b) The current IR at AC bus under the SC short circuit fault.

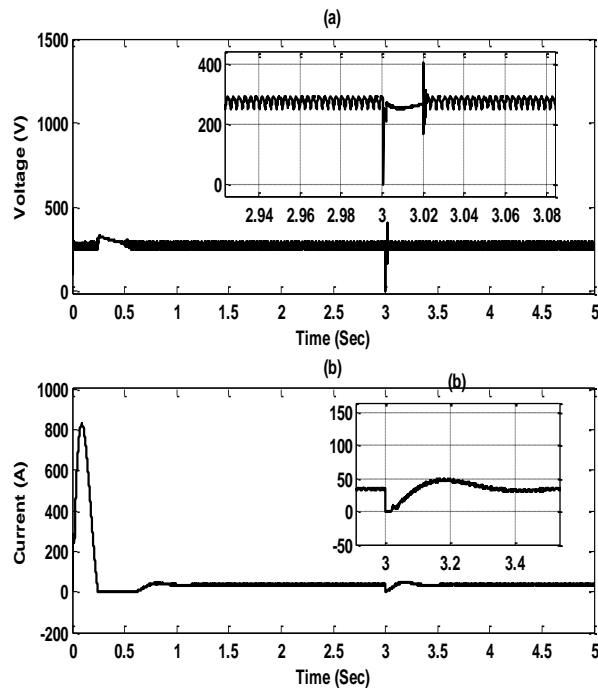


Fig.29. (a) The Voltage VR at AC Bus under the open circuit fault. (b) The Current IR at AC Bus under the OC open circuit fault.

5. CONCLUSION AND FUTURE WORK

The paper presents a two-stage multi-level fuzzy control structure with two novel Green plug-switched filter compensators on the AC and DC sides of a decoupled energy efficient hybrid AC-DC energy efficient decoupled hybrid drive-battery charging scheme fed from AC Grid with a PV array added for battery charging. This novel approach reduces the fuzzy rule numbers but still maintains the linguistic meaning of fuzzy variables. The modified two stage fuzzy logic controller is validated for effective reference speed tracking under different speed trajectories under both normal and excursion conditions with photovoltaic source variations and load excursions. The decoupled multi-loop error driven, de-scaled HFLC controller was very effective in damping all excursions and parameter variations. Future work will consider using fuzzy decision trees to analyze the sensitivity of the fuzzy rules to different antecedents and develop an automatic method of searching for the intermediate variables, rather than relying on expert knowledge. Online adaptation of hierarchical fuzzy rules is also to be investigated. The new use of green plug on DC side and SFC filter on the AC side ensures less ripple and fast dynamic operation and motor control with less ripple as well as battery fast charging. The two new designs are now being extended to renewable energy PV-Wind-Tidal-Micro Hydro-Fuel Cell-distributed multi-source micro grid energy systems and future EE-Energy Storage use in Smart –Grid distribution and smart Building-utilization as well as large electric drives. The proposed multi-stage-multi regulation multi loop error driven weighted time de-scaled and decoupled control structures is being validated in electric vehicles and AC and DC large drive systems.

Appendix 1: Values of used variables and factors

PMDC Motor:	$\gamma_{Vd}=1$
$R_m = 0.08\Omega$	$\gamma_{Id}=0.5$
$L_m=0.0012H$	$\gamma_{VB}=1$
$J = 0.12Kg \cdot m^2$	$\gamma_{IB}=0.5$
$B = 0.02N \cdot m \cdot s$	GPFC Parameters:
$K_e = K_t = 0.5835N.m/A$	$R_f = 0.15\Omega$
Battery parameters:	$L_f = 10e-3H$
Nominal Voltage=300 V DC	$C_s = 250\mu F$
Rated Capacity=1250 Ah	$C_d = 5500\mu F$
Max Capacity=1250 Ah	Buck-boost Parameters:
Fully Charged V=349.2V DC	$R_o = 0.05\Omega$
Nor. Discharging Current=543.5A	$L_o = 5e-3H$
Internal R=0.0024 Ω	AC Side:
Capacity@Nor.V. =1130.4	$V_S = 11KV$
Expon. volt. zone=324.116V	S.C. Level = 50MVA
Initial SOC=50%	Transformer 11Kv/208V
Expon. Capacity zone=61.4Ah	Modified PIDFLC Controller:
Auxiliary DC Load 50Kw	$\gamma_e=0.5$
Auxiliary PMD Motor 60Kw	$\gamma_R=1$
Dual-loop Controller	$K_p = 25$
$\gamma_{VR}=1$	$K_I = 10$
$\gamma_{IR}=0.5$	$K_d = 2$

References

- [1] A. Luis, V. Lara, L.V. José-Brito, and Y. Valencia. Comparative analysis of semi-active control algorithms applied to magnetorheological dampers, *Ingeniare. Revista chilena de ingeniería*, 25(1), 39-58, (2017).
- [2] F. A. Salem, M. K. Mohamed, and U.H. Issa, Proposed Simple and Efficient Control Algorithm Design Approach, *International Journal of Applied Engineering Research*, 12(9), 2044-2053, (2017).
- [3] N. Baćac, V. Slukić, M. Puškarić, B. Štih, E. Kamenar, and S. Zelenika, Comparison of different DC motor positioning control algorithms, *MIPRO/SP*, 1895-1900 (2014).
- [4] A-F. Attia, H. Soliman, and M. Sabry, Genetic algorithm-based control system design of a self-excited induction generator, *Acta Polytechnica*, 46 (2), 11-22, (2006).
- [5] G. Shabib, M. A. Gayed, and A. M. Rashwan, Optimal tuning of PID controller for AVR system using modified particle swarm optimization, In *Proceedings of the 14th International Middle East Power Systems Conference (MEPCON'10)*, Cairo University, Egypt, (2010).
- [6] Z. L. Gaing, A Particle swarm optimization approach for optimum design of PID controller in AYR System., *IEEE Energy Convert*, 9(2), 384-391, (2004).
- [7] A. Bagis, Tabu search algorithm based PID controller tuning for desired system specifications, *Journal of the Franklin Institute*, 348, 2795–2812, (2011).

- [8] Z. Yachen, Hu Yueming, On PID controllers based on simulated annealing algorithm, In. Proc. of the 27th Chinese Control Conference, china, (2008).
- [9] M. Abachizadeh, M. Yazdi, A. Yousefi-Koma, Optimal tuning of PID controllers using artificial bee colony algorithm, IEEE/ASME ICAIM:379–384, (2010).
- [10] G. Murugananth, S. Vijayan, J.S. Alexis, and S. Muthukrishnan, A Comparative analysis of PI, PID and anti-windup PI schemes for PMDC motors. Int. J. Comput. Appl. T. 57(2), 21-25, (2012).
- [11] A. -F. Attia, Hierarchical fuzzy controllers for an astronomical telescope tracking, Applied Soft Computing, 135-141, (2009).
- [12] V. Tipsuwanpornm, T. Runglimmawan, S. Intajag, and V. Krongratana, Fuzzy logic PID controller based on FPGA for process control, IEEE-ISIE, Vol. 2, 1495-1500, (2004).
- [13] Z. Stevic, and I. Radovanovic, Energy efficiency of electric vehicles. INTECH, Chapter 4, (2012).
- [14] P.K. Olulope, and K.A Folly, Comparative analysis between synchronous wind generator, small hydro power, solar PV and hybrid power system for distributed generation applications, IJARER, 1(11), 642-648, (2012).
- [15] S. Sumathi et al., Solar PV and wind energy conversion systems. Springer International Publishing Switzerland, Chapter 2, (2015).
- [16] K. Sivakumar, and D. A. Vijula, Traction assistance system for four wheel drive electric vehicle, International Research Journal of Engineering and Technology, 1(2), (2015).
- [17] A. Nasri et, and B. Gasbaoui: Neuro-Fuzzy control for four Wheels electric vehicle safety, Revue des Energies Renouvelables, 20(1), (2017).
- [18] E. Elbakush, A.M. Sharaf, and I. H. Altas, An efficient tri-loop controller for photovoltaic powered four-wheel electric vehicle, IEEE: 421-425 (2008).
- [19] A. M. Sharaf, A. El-Gammal, A hybrid PV-FC-diesel-battery electric vehicle drive system based on PSO self-regulating multi-loop incremental controller, 16th National power systems Conference, India, 435-440, (2010).
- [20] D. Sharma, P. Gaur and A.P. Mittal, Performance analysis of a photovoltaic and battery powered electric vehicle with PMSM motor drive, Impending Power Demand and Innovative Energy Paths, 101-107, (2015).
- [21] A. E. Gegov, P. M. Frank, Hierarchical fuzzy control of multivariable systems, Fuzzy Set System, 72(3), 299-310, (1995).
- [22] A. M. Sharaf, R. Chhetri, A novel dynamic capacitor compensator/green plug scheme for 3-phase 4-wire utilization loads. IEEE-CCECE, Ottawa, Ontario, Canada, (2006).
- [23] A. M. Sharaf, A. Aljankawey, and I. H. Altas: A novel voltage stabilization control Scheme for stand-alone wind energy conversion systems. Proc. Conf. Clean Elect. Power, 514-519, (2007).
- [24] A. M. Sharaf, M.Z. El-Sadek, F. N. Abd-Elbar, A. M. Hemeida, A global dynamic error driven control scheme for static VAR compensators, EPSR, 51 (2), 131-141, (1999).
- [25] E. Elbakush, and A. M. Sharaf, A hybrid FACTS PV-smart grid (V2G) battery charging scheme, IJARER, 1(10), 560-572, (2012).
- [26] A-F. Attia, A. M. Sharaf, A Robust FACTS Based Fuzzy Control Scheme for Dynamic Stabilization of Generator Station, Ain Shams Engineering Journal, (In press) (2019).
- [27] A. M. Sharaf, and A. El-Gemmal, A hybrid PSO-self-regulating VSC- SMC controller for PV-FC-diesel-battery renewable energy scheme for buildings electricity utilization, 2010 Fourth Asia International Conference on Mathematical/Analytical Modeling and Computer Simulation, 463–469 (2010).
- [28] A-F. Attia, Online Tuning Based Fuzzy Logic Controller for Power System Stabilizers, 19th International Middle East Power Systems Conference (MEPCON'17), 19-21 December 2017, Cairo, Egypt.
- [29] A-F. Attia, A. M. Sharaf, A Novel Multistage Fuzzy Controller for FACTS Stabilization Scheme for SMIB AC System, 16th International Middle East Power Systems Conference (MEPCON'14), 23-25 February 2014, Cairo, Egypt.

Biographies



Abdel-Fattah Attia graduated from Mansoura University in 1991 and obtained his M. Sc. from Ain Shams University, 1997, Cairo, Egypt and the Ph.D. degree in Control Engineering and Robotics from Czech Technical University in Prague, Czech Republic, 2002. Dr

Attia is the Founder and Head of ISRG Group & Vice Dean for Graduate Studies & Research at Faculty of Engineering, Kafrelsheikh University. Dr. Attia has more than 45 scientific research papers published in prestigious international journals. He co-supervised 9 graduate students (3 Ph.D., and 6 M.Sc. students) at Ain Shams University. His research interests include the development, modelling and identification of nonlinear systems, fuzzy models, neural networks, neuro-fuzzy and genetic algorithms.

E-mail: aheliel@eng.kfs.edu.eg



Adel M. Sharaf obtained his B.Sc. degree in Electrical Engineering from Cairo University in 1971. He completed a M.Sc. degree in Electrical engineering in 1976 and Ph.D. degree in 1979 from the University of Manitoba, Canada and was employed by Manitoba

Hydro as Special Studies Engineer, responsible for engineering and economic feasibility studies in Electrical Distribution System Planning and Expansion. Dr. Sharaf was selected as NSERC-Canada Research-Assistant Professor in 1980 at University of Manitoba. He joined the University of New Brunswick in 1981 an Assistant professor and he was promoted to Associate

Professor in 1983, awarded tenure in 1986, and the full professorship in 1987. Dr. Sharaf has extensive industrial and consulting experience with Electric Utilities in Canada and abroad. He authored and co-authored three book chapters, over 700 scholarly technical journals, refereed conference papers and engineering reports. He supervised over (51) Graduate students (37-M.Sc. &14-Ph.D.) since joining academia in July-1981 on the subjects of power systems control, stability, protection, power quality, renewable green-energy, electro-technology and environmental devices.
E-mail: profdramsharaf@yahoo.ca



Fathalla Selim was awarded with Bachelor in Electrical Engineering in 1997 and obtained his M.Sc. from Alexandria University, 2007, Alexandria, Egypt and the Ph.D. degree from Tanta University, Tanta, Egypt, 2012. Dr. Fathalla Selim is the coordinator for post-graduate studies in Electrical Power

and Machines Department, Faculty of Engineering in Kafrelsheikh University. Dr. Fathalla Selim is electrical consultant engineer in Engineering Syndicate, Egypt. Fathalla has more than 20 scientific research papers published in international journals and conferences. His research interests include the development, modeling and identification of nonlinear systems, and economic generation and consumption power algorithms and advanced techniques.

E-mail: hegaz2009@yahoo.com